DEGREE MASTER PROGRAMME IN ELECTRICAL ENGINEERING

MASTER'S THESIS

Digital modulation and 3D printing - new techniques to be exploited in near-infrared spectroscopy of the brain

Author	Iván Ruano Jiménez
Supervisor	Teemu Myllyla
Second Examiner	Vesa Korhonen
Technical Advisor	Erkki Vihriälä

September 2018

Ruano I. (2018) Digital modulation and 3D printing - new techniques to be exploited in near-infrared spectroscopy of the brain. University of Oulu, Degree Programme in Master of Electrical Engineering.

ABSTRACT

The brain, one of the main organs in the human body, has been extensively studied throughout the history of medicine. Some brain parameters, particularly the hemodynamic parameters, are associated to several brain disorders. Due to this connection, NIRS (Near infrared spectroscopy) techniques play a key role in brain research – they measure such parameters in order to potentially exploit the early-detection process. NIRS devices make use of near infrared spectrum, light between 650nm and 950nm, to measure various parameters non-invasively and changes of the tissue such as concentrations of oxy-(HbO2) and deoxyhaemoglobin (HbR) - main absorbers of most tissues in this spectral range and related to blood oxygenation and volume changes.

TM-NIRS, CW-NIRS and FD-NIRS combined with code-modulation techniques are commonly used for medical purposes. Nowadays, new modulation techniques for wireless communication are being developed and could be even used in NIRS techniques. Based on this fact, this thesis provides a review of existing NIRS modulations and discusses their strengths and weaknesses.

The main aim was to build a new simple, affordable, and operative NIRS transmitter that can be utilised in digital modulation techniques focusing on human and mice measurements. In addition, this project was aimed to exploit 3D printing sensor design techniques and the testing process of the designed device. A 4kHz emitter with 4 high-power LEDs, a clock signal generator, decade counters and a receiver was designed and tested. Furthermore, PPG signal-NIRS optodes and a prototype of a phantom head were designed and 3D printed.

Key words: NIRS, 3D printing, modulations, phantom head.

TABLE OF CONTENTS

FOREWORD

First of all, I would like to thank Dr. Teemu Myllylä for his unconditional support. Without his knowledge and patience, I would not have been able to carry out and complete this thesis. I would also like to express my gratitude to Msc. Erkki Vihriälä for all the help I received in the day-to-day work in the laboratory. His advice and recommendations regarding laboratory techniques made me expand to a great extent my knowledge about electronics. And last, but not least, I would like to thank Msc. Jaakko Hakala. His work experience played an important and useful part during the difficult times of the project.

Thank you to every single person I have met in Oulu. I will carry you and this experience in Finland deep in my heart.

Oulu, September, 27 2018

Iván Ruano Jiménez

LIST OF ABBREVIATIONS AND SYMBOLS

NIRS	Near infrared spectroscopy
Hb	Hemoglobin
HbR	Deoxyhemoglobin
HbO_2	Oxyhemoglobin
CW	Continuous wave
FD	Frequency domain
TD	Time domain
TDMA	Time domain multiple access
FDMA	Frequency domain multiple access
CDMA	Code division multiple access
SNR	Signal to noise ratio
VCSEL	Vertical-cavity surface-emitting laser
PGA	Programmable-gain amplifier
ADC	Analog-to-digital converter
RF	Radio frequency
LO	Local oscillator
IF	Intermediate frequency
PLL	Phase-locked loop
VCXO	Voltage-controlled crystal oscillator
EEG	Electro-encephalography
MEG	Magneto-encephalography
fMRI	Functional magnetic resonance imaging
TCD	Transcranial Doppler
CBF	Cerebral blood flow
BOLD	Blood-oxygen-level dependent
BBB	Blood brain barrier
CNS	Central nervous system
MEMS	Microelectromechanical systems
SMD	System mounted device
tHb	Total haemoglobin
TOI	Tissue oxygenation index
PPG	Photoplethysmogran

I	Intensity before light enters materia
I_o	Intensity after light transmission
c	Concentration of the chromophore
l	Mean of the light path
A	Measured attenuation
C	Chromophore concentration

L	Differential path length
$\boldsymbol{\varepsilon}$	Molar absorptivity of the target chromophore
$\boldsymbol{\lambda}$	Wavelengths

1. INTRODUCTION

1.1. Motivation

Over the years, Neuro-investigation has been of great interest for the scientific community. A large amount of money and time have been invested aiming at learning more about the nervous system, about how it works, how it communicates with other mechanisms of the human body, and what cause diseases related to its running.

New optical techniques have been developed to complement and improve traditional neuroimaging systems, allowing the research and development of new methods in early detection of diseases of the nervous system. NIRS devices have meant a great advance in this field and hospitals are beginning to implement them. By doing this, they complement the use of traditional neuroimaging techniques including EEG, MEG or MRI to early detection of diseases such as dementia or brain edema.

Therefore, it is important to continue with the development of NIRS techniques and processes and utilize new fabrication techniques, particularly 3D printing. This type of printing provides the possibility, among others, of designing optimized shapes of optodes.

It is important to note the importance of preliminary experiments during medical human researching processes where mice measurements play a major role. As a consequence, one of the main purposes of this thesis is to develop a new NIRS transmitter that can be applied in both human and mice studies.

1.2. Objectives

The purpose of this thesis was to design and create a new, affordable, simple and functional NIRS transmitter that met the necessary specifications required in mice and human measurements. It is also intended to exploit the development of 3D printing technology to design and build pieces that facilitate some of the optical systems used in biomedical researching. The objectives were divided as follows:

- Introduce the current art of NIRS systems
- Design and create a functional and affordable NIRS switching system hardware
- Design and create 3D printing pieces for easing biomedical studies
- Testing of new NIRS transmitter in technical laboratory with the aim of be used in future mice experiments

1.3. Outline of thesis

Firstly, chapter two shows a study of the current art of NIRS devices. Here, the operation existing methods and modulations are explained, along with the implementation in multimodal studies in medicine researching field.

Secondly, the process of designing the NIRS system is described including the explanation of the transmitter and likely cases that may arise when building the switching system. The option chosen and the operation are detailed together with the used components and the manufacturing process. This process is similar to the case of

the receiver, where the specified design and its operation are addressed. The results obtained in the testing process of the system are also specified.

Point 4 of the project addresses 3D printing with the purpose of creating pieces for biomedical projects. Specifically, PPG signal measurement systems and the process of designing and manufacturing an optode are explained. In addition, the current state-of-the-art of phantom heads for biomedical testing with microwaves, as well as optical systems and the process of designing and manufacturing a scale model of a human head mould for testing, are detailed.

1.4. Schedule

This project has a duration of approximately 6 months, in which the tasks have been distributed as shown in the following diagram:

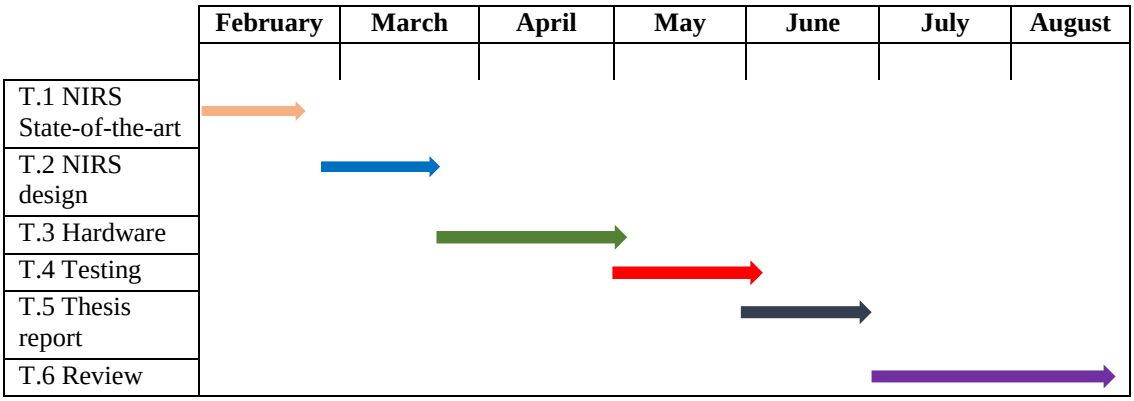

Table 1: Time diagram

TASK	NIRS State-of-the-art documentation	New NIRS system design	Hardware fabrication	Testing and corrections	Thesis report	Thesis review and mice measurements
DURATION	1 February – 22 February	26 February – 19 March	21 March – 1 May	2 May – 30 May	1 June – 27 June	28 June – 31 August

Table 2: Time table

2. NIRS STATE-OF-THE-ART

The brain is the central organ of the human nervous system and, as a result, medical research has mainly focused on the study of the brain activity for decades. It is essential to develop non-invasive techniques that allow the measurement of some significant parameters such as brain water content, pulse oximetry or dynamics in oxyhaemoglobin, for instance. In this context, NIRS plays a key role regarding early detection of several brain conditions. Thus, a basic NIRS system was developed in addition to new 3D designs that served to test the NIRS device and ease the measurements of various brain parameters using parallel optical techniques.

2.1. Development of NIRS devices

Near-infrared spectroscopy (NIRS) is a technique that uses near-infrared (NIR) (light between 650nm-950nm) to measure different parameters of the tissue non-invasively. The origins date back to the forties, decade where the muscle oximeter was invented by Glenn Millikan [1]. This technique has evolved over the years to this day and has achieved great results.

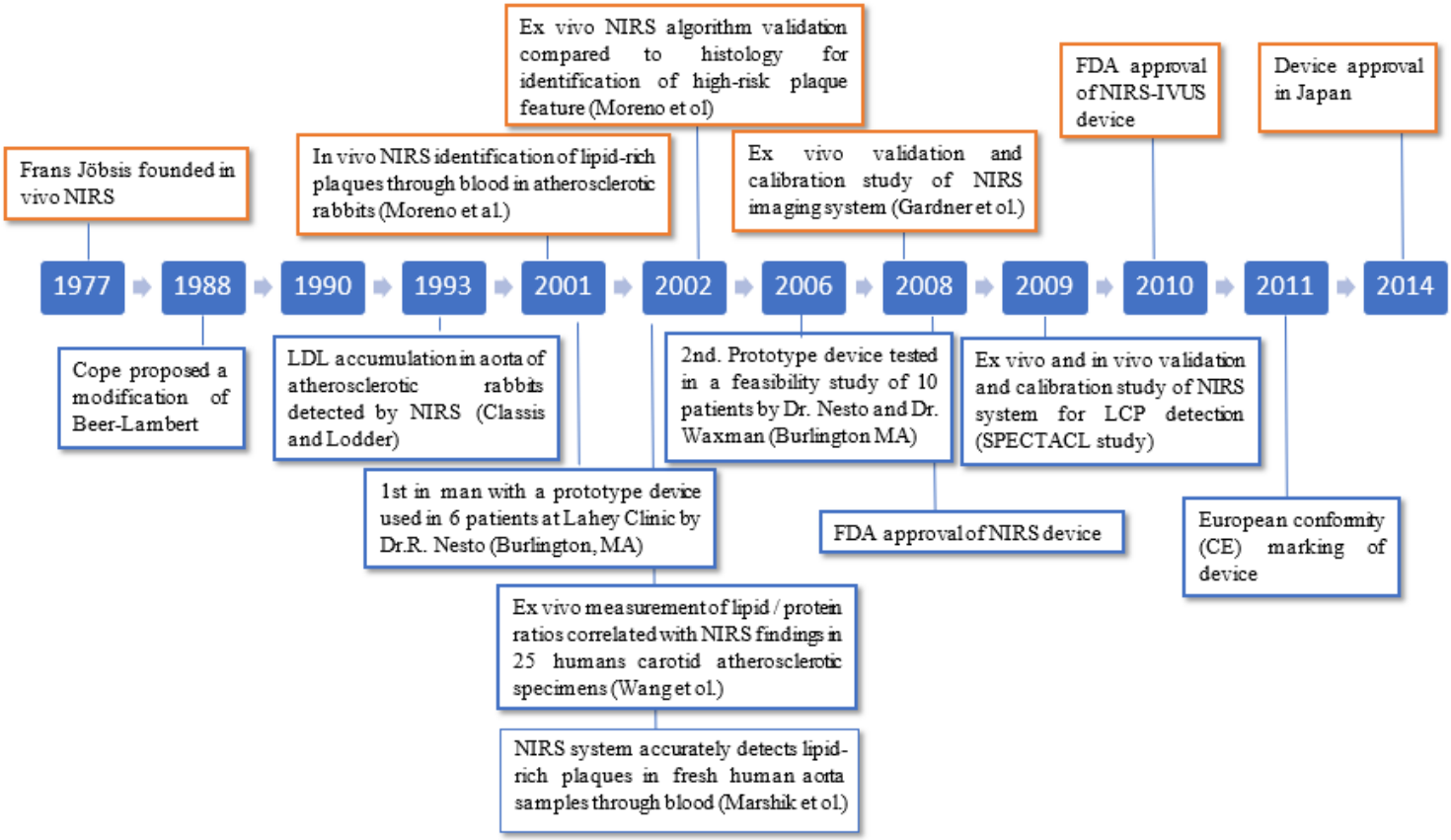

Figure 1: Evolution of some NIRS achievements from 1977 to 2014 [2]

Brain activity is associated with several physiological events, some of which are equally associated with changes in the optical properties of brain tissues. Optical methods have a considerable number of strengths including temporal resolution in mm or the potential to measure intracellular/intravascular events simultaneously [1].

In 1977, Frans Jöbsis, founder of in vivo NIRS, reported, after moving to the Department of Physiology of Duke University, that the relatively high degree of brain tissue transparency in the NIR range enables a real-time non-invasive detection of haemoglobin oxygenation using transillumination spectroscopy [1].

Some years later, in 1980, Marco Ferrari started using NIRS instrumentation prototype to measure brain oxygenation changes in experimental animal models and human adults. These studies showed interesting data such as the effects of carotid artery compression on regional cerebral Hb oxygenation and the volume of cerebrovascular patients [1].

In 1988, Cope proposed a modification of Beer-Lambert Law that would allow the quantification of brain absorption changes within absorbing samples and a differential path-length factor.

Between 1980 and 1995, several companies developed NIRS prototypes and demonstrated that NIRS techniques were one of the most important advances in neuroscience.

Light absorption changes of some exposed animals in response to visual stimulation were studied. After achieving successful results, Chance and his team started to make use of the NIRS with a cognition-activated low-frequency modulation technique to measure light absorption in human brain incorporated. These events led to the apparition of the FD NIRS in 1993.

Not before 1996 was it possible to find the first single channel TD NIRS designed by Obrig [4] and multichannel TD NIRS designed by Cubeddu and his team a few years later [5].

After years of research of NIRS techniques, a functional NIRS was developed. This technique offers a non-invasive, safe, portable and low-cost method of monitoring cerebral blood flow, among other characteristics. This is possible through the measurement of changes in concentration of oxy- and deoxy-haemoglobin in relation with the specific optical spectrum between 700-1000nm.

As shown in Figure 1, progress in NIRS techniques and neuroimaging have been indispensable and, nowadays, these neuroimaging techniques are commonly used in researching areas of hospitals around the world.

A key figure in the development of NIRS techniques is David Boas. By studying side by side with medical experts, Boas and his team have utilised NIRS techniques to study brain development in infants, finding that neurophysical correlates language development. Besides, they have consolidated NIRS-fMRI techniques, that stablish a biological basis of the fMRI bold signal, and further multimodal techniques including NIRS-EEG/MEG used to study hemodynamic responses of brain activity.

2.2. Near-infrared spectroscopy (NIRS)

As mentioned above, NIRS is a spectroscopic technique that measures relevant parameters through the near-infrared light not only in neuroscience, but also in sports medicine, food or pharmaceutical.

One of the key features of NIRS is the unique absorption characteristics of each chromophore. Therefore, detector signals can be un-mixed to quantify the amount of chromophore in a tissue. Traditionally, NIRS has been put to use to monitor changes in amounts of oxy-(HbO_2,) and deoxyhaemoglobin (HbR) - main absorbers of most tissues in this spectral range that are related to blood oxygenation and volume changes. Another relevant factor is the scattering effect of NIR light in tissues since, in most cases, it is more probable than absorption. It is a fact that scattering increases the mean pathlength of photons, so this do necessary to measure both, mean pathlength and attenuation, and separate then absorption and scattering properties of the medium to get a good quantification of NIRS [6].

By applicating NIRS, light is processed through the brain tissue after its transmission. Due to the scattering nature of NIR light in tissues, variability in detected signals cannot be simply attributed to changes in chromophore concentration and a computational reconstruction is required [7].

The basic law that relates the attenuation of light to the properties of the material through which the light is travelling is referred to as Beer-Lambert law:

$$log\,\frac{Io}{I} = \varepsilon lc \tag{1}$$

ε is the molar absorptivity of the target chromophore, I is the intensity before and after the transmission of light and c is the derived concentration of the chromophore.

The Beer-Lambert law assumes that all light is transmitted and not scattered, reason why a new modified Beer-Lambert law was developed by Delphy in 1988. This new law considers differential path lengths (L) and attenuations measured at multiple wavelengths (A) [7]:

$$\begin{bmatrix}\Delta C_1\\ \Delta C_2\end{bmatrix} = \frac{1}{L}\left[\varepsilon_{I,J}\right]^{-1}\begin{bmatrix}\Delta A(\lambda_1)\\ \Delta A(\lambda_2)\\ \Delta A(\lambda_3)\end{bmatrix} \tag{2}$$

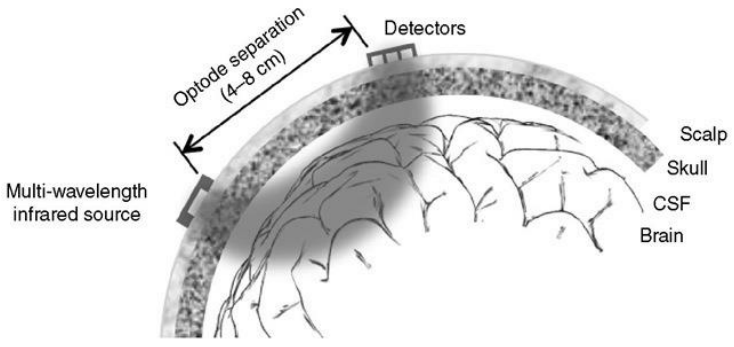

Figure 2: Diffuse path of light due to scattering [8]

2.3. Types of methods

Whereas modelling is a relevant factor regarding the accuracy of NIRS, good quality measurement detections are just as important. Nowadays, there are three different detection modes in NIRS: Continuous Wave (CW), Frequency Domain (FD), Time Domain (TD) and Code-Division Multiple Access (CDMA). Example of the different input and output signals in different modes are shown in Figure 3.

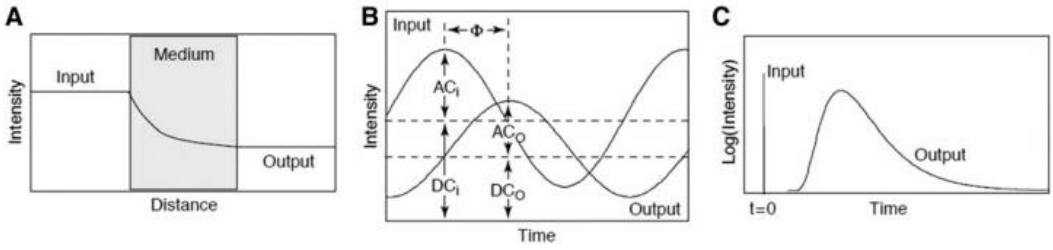

Figure 3: A-CW signals, B-FD signals and C-TD signals. [6]

2.3.1. CW NIRS

CW instruments are the first-invented and most simplistic instruments. Their only function is to measure the attenuation of the input light due to non-existing or low modulation of the light. This is a fast and relatively low-cost method, but it does not provide absolute measurements [7]. They are the most commonly used devices and can be combined with multichannel configurations or derive quantitative values such as tissue oxygen saturation [8].

These devices have three main access modulation methods, through which multiple laser signals, detected by the same detector, are distinguished: TDMA (Time-Division Multiple Access), FDMA (Frequency-Division Multiple Access) and CDMA (Code-Division Multiple Access).

TDMA modulation consists of emitting every source in slots (time divisions). This method could be easily implemented, nevertheless, SNR and time-domain resolution are still not optimal [9].

FDMA is a common modulation in conventional NIRS systems [9]. The laser sources are modulated through orthogonal frequencies and, consequently, this hardware is more not as easy compared to other techniques. Another issue involved is the degradation caused by nonlinearities of the sources.

CDMA uses orthogonal codes and achieves to not be affected by analog-domain signal integrity. This type of coding allows to get a maximized SNR in the receiver with a simple digital-domain matched filter and a good immunity from frequency interference [9].

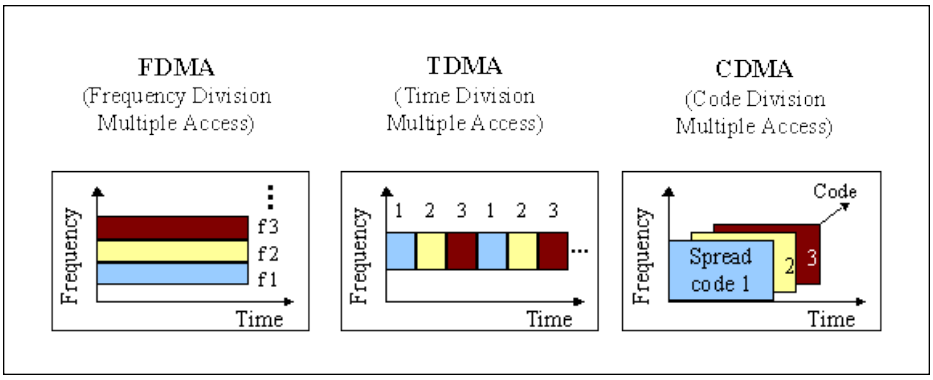

Figure 4: CW Modulations [9]

Figure 5 shows an example of a CDMA NIRS system and how the laser source is driven by an orthogonal Walsh code. The detectors receive combined light signals with information about hemodynamics from the different regions. Due to the fact that the propagation speed of light in the brain is smaller than the code rate, the detected signal is synchronized with the original one and, for that reason, it is not necessary to include a timing-recovery circuit [9].

Regarding the light sources, VCSEL lasers are in charge of modulating with the CDMA code. Light detection is performed through silicon PIN diodes with a transimpedance amplifier (TIA), converting current into voltage. Other essential devices are PGA and ADC.

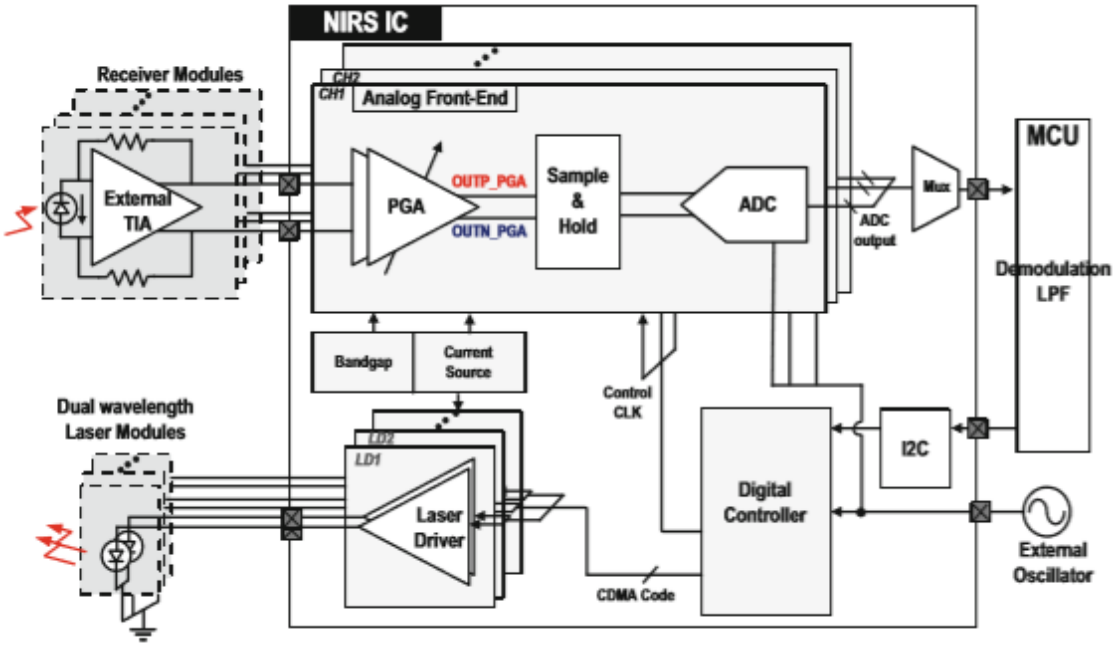

Figure 5: Example of block diagram of CDMA NIRS [9]

As mentioned above, CW NIRS provides non-invasive techniques to measure relative changes in oxy and deoxy-haemoglobin. This allows to, for instance, determinate the local skeletal muscle O_2 saturation, muscle oxygen consumption or blood flow [10].

2.3.2. FD NIRS

Regarding FD technique, the light of the sources is modulated at radio-frequency (>50MHz). The measurable parameters are the modulation amplitude, the average intensity and the phase shift.

It is interesting to note that at frequencies <200MHz, the measured phase shift is proportional to the mean pathlength of the photons of the tissue.

By measuring all frequencies, the information between TD and FD techniques is similar. Nevertheless, this information would have a high complexity in FD case and a lower dynamic range and repeatability. However, with a single-frequency measurement of the modulation amplitude and phase, it is possible to resolve the absorption in tissue. Therefore, single-frequency FD techniques should be considered [6].

Figure 6 shows an example of a block diagram belonging to a FD system. This instrument is composed of four laser diodes modulated at 100 MHz biased with current sources and modulated with a signal generator. A 4x1 fibre-optic MEMS switch is used to select a single source wavelength and a 1x16 MEMS switch to select one active position. The light is detected through 16 parallel photo-multiplier tubes [6].

The received RF signal is amplified and combined with a LO, producing a 5kHz signal. Once the combination is completed, a low-pass filter is introduced and the signal is guided to an IF amplifier. In this case, after this process, the signals are sampled with both parallel 8-channel data acquisitors using a 20kHz sampling frequency [6].

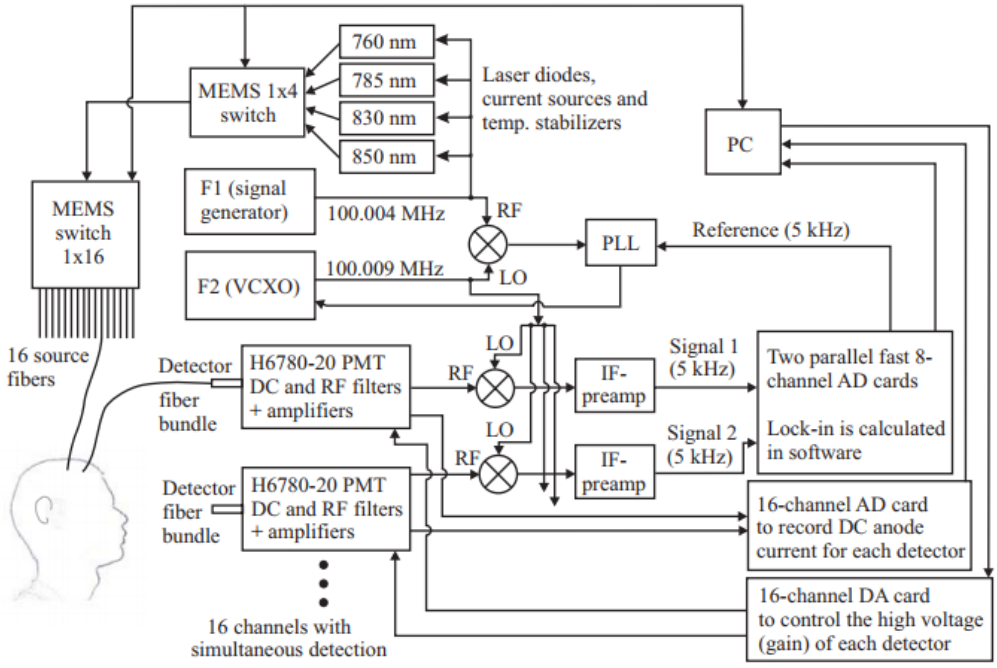

Figure 6: Example of diagram block in FD technique [6]

In order to ensure high-accurate measurements, a heterodyne with phase-lock loop (PLL) detecting system was selected. The PLL adjusts the frequency difference between the VCXO and the signal generator with the purpose of matching them. After this procedure, the phases of all measurements are synchronized.

This block diagram could represent a good example of how to utilise FD NIRS since this prototype was introduced in hyperventilation and breath-holding studies to induce hemodynamic and oxygenation changes in the brain.

2.3.3. TD NIRS

In this technique, short light picoseconds are introduced into the head and broadened and attenuated by the different tissue layers. The spread point function of the photons that leave the tissue is used to identify changes in attenuation and optical path length [11].

TD technique detects ballistic and diffused scattered photons. Unfortunately, this technique requires a high budget, along with great averaging times to obtain a good SNR. Furthermore, these techniques are usually of great size and not suitable for clinical monitoring [6].

TD NIRS can be applied in different ways, but one remarkable way would be the monitoring of muscle oxidative metabolism. This application is relevant for the training status of athletes and the rehabilitation process for different patients [12].

2.4. NIRS in multimodal brain research

The use of multimodal measurements to study the mechanisms and relationships among different activities, electrophysiology or blood-flow in brain researches is meaningful. At this point, it is important to explain the simultaneous use of functional near-infrared spectroscopy (fNIRS) and different functional neuroimaging modalities as EEG, MEG or fMRI.

For instance, varieties of measurements have been executed by the Oulu University, who applied multimodal brain imaging to measure blood pressure and cardiorespiratory oscillations, or by the University of Calgary, who applied NIRS techniques in combination with MRI to study brain oxygenation and metabolism.

2.4.1. Functional imaging of the brain

The technical parameters of the most relevant techniques in neuroimaging are briefly explained here:

- **EEG**: This technique has a high temporal resolution (ms) that follows brain activity changes, and yet a relatively modest spatial resolution (cm). This spatial resolution constitutes a weak characteristic since localizing brain functions precisely in brain studies is essential. There are many applications of EEG in the field of research, including human factors studies, psychology and neuroscience, psychiatric studies, brain computer interfaces…

- **MEG**: It measures the magnetic fields of the body currents. It has a temporal resolution of less than 1 ms and a spatial accuracy of few mm. This technique is commonly used for detecting and localizing pathological activity in patients that suffer from epilepsy, eloquent cortex for surgical planning in patients with brain tumours or intractable epilepsy, among others pathologies.

- **MRI**: It is a non-invasive technique based in nuclear magnetic resonance. Its aim is to obtain information regarding the structure and composition of different tissues. It is widely applied in all medical fields for studying different conditions: prostate cancer assessment, breast MRI, cardiovascular system, complex neuro imaging…

Currently, fMRI dominates in brain mapping applications due to its high spatial accuracy and lack of radiation exposure. Nonetheless, its time resolution is poor and other techniques as MREG are being used instead. MREG offers a time resolution of 0.1s - 0.06s - an ultrafast fMRI that allows the observation of functional signal in the brain at low frequency, filtering physiological noise and detection of single event activations [13]. When applying fMRI, the patient must be in a lying position and stay still during the measurements, all of which constitute additional weaknesses. fNIRS has benefits respecting the regression of low-frequency noise from MRI since NIRS measures physiological fluctuations with higher temporal resolution. Moreover, fNIRS receives information of both HHb and HbO_2 in addition to HbT changes, whereas fMRI is only sensitive to changes in HHb and blood flow. In conclusion, NIRS improves physiological interpretation of fMRI and it is applicable to mobile measurements. Therefore, the combination with other techniques would be interesting [14].

The mechanisms that link cardiovascular and brain functions have a strong emphasis. For this purpose, it is crucial to develop multimodal methods that combine accurate blood pressure measurements and assessments of cerebral hemodynamic. Some innovating techniques including the transcranial Doppler have provided the opportunity to determine CBF velocity in intracranial arteries. Doppler ultrasound beam penetrates the temporal bone and, in most cases, reaches the circle of Willis. In addition, ultrasound provides an accurate estimation of red blood cell velocity in these vessels [14]. However, this technique has 3 big limitations:

- 30% of old and female patients have poorly penetrable temporal bones
- Researches limit the confirmation of vessel diameter stability
- In many cases, blood vessel is not visible during the measurements

Functional NIRS has the potential to complement TCD recordings of CBF considering that the spatial resolution of TCD is not as good as expected. The TCD records the changes in blood flow in MCA, but it does not locate them. As opposed to this, NIRS provides the required information by measuring cerebral cortical tissue oxygenation in the brain or in some specific areas. However, it is equally limited and does not analyse the whole brain. Some research works have applied a set-up based in 4 NIRS optodes integrated with a Spencer TCD headgear in order to study effects of orthostatic hypotension on brain perfusion during changes in body position, among other applications [14].

2.4.2. Examples of NIRS in multimodal set-ups

Materials in MRI rooms must be handled with caution due to the presence of a large static magnetic field, reason for prohibition of ferromagnetic materials.

As to the NIRS device, optical fibres and optodes must be non-magnetic, otherwise it would attach itself to the head inside the MRI scanner if it is close to it. In the same way as MRI, any material used near the MEG scanner must be non-magnetic and electronic devices are not allowed inside a MEG room, only the ones made of passive components. In the case of NIRS, only plastic optical fibres are allowed in the MEG room [14].

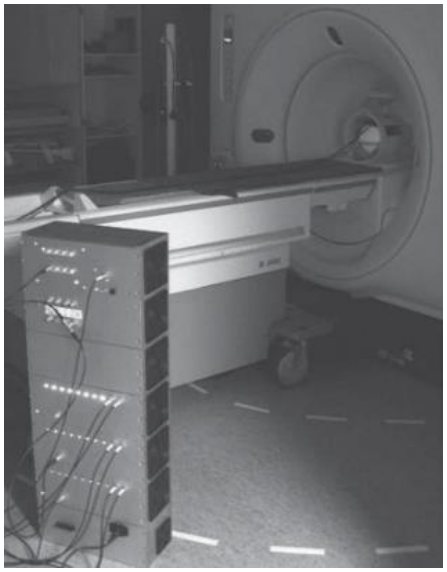

Figure 7: MR-compatible NIRS device in a 1.5-T MRI room [14].

The combination between NIRS and fMRI provides accurate anatomical information regarding the brain that enables the estimation of light propagation in the head. NIRS is beneficial to the regression of low-frequency physiological noise from fMRI data since its temporal resolution is higher. Moreover, fNIRS measures HHb, HbO2 and HbT changes whereas fMRI is sensitive to HHb and blood flow exclusively. NIRS also enables the measurement of mitochondrial cytochrome activity, which, in combination with fMRI, means a new method for studying the connection between metabolism and oxygenation [14].

While functional NIRS and MRI are hemodynamic techniques, EEG is sensitive to integrated neuronal activity. The main issue, as mentioned before, is the low spatial resolution due to the effects of the skull and tissue on electric fields. Given that cerebral hemodynamic changes and neuronal activities are related through the neurovascular coupling, simultaneous application of EEG and NIRS is an efficient method to study the brain.

Similar to EEG, MEG is sensitive to the activity in the pyramidal cortical neurons, but unlike EEG, MEG's spatial resolution is more advanced. The combination MEG/NIRS implies a more effective tool to study the brain. Unfortunately, this system is high-priced and, consequently, the studies are constrained. Moreover, some recent

studies show that MEG could potentially measure both neuronal and hemodynamic functional brain signals [14].

Lastly, a perfect illustration of a multimodal set-up can be found in the Medical Research Center of Oulu. This technique consists of non-invasive, simultaneous and continuous blood pressure fluctuation, as well as pulse propagation, changes in respiration and brain and heart electrical activity and hemodynamic measurements. The fMRI set-up utilises MREG imaging technique, which makes unaliased sampling of BOLD signals possible. Several sensors that receive the information are attached to the subject. This set-up enables the study of diverse brain disorders such as epilepsy, narcolepsy, autism spectrum disorders or monitoring treatment of central nervous system lymphoma that involves brain barrier disruption. To monitor BBB, Oulu University proposes the EEG+NIRS method for human beings during CNS lymphoma treatment. In the near future, this method may also be combined with ultrafast MRI and monitor BBB integrity from deep brain structures [15] [16].

3. NIRS DEVICE DESIGN

As it has already been said, NIRS techniques are starting to be commonly applied in hospitals all over the world. For this reason, a new affordable, portable and easily-used NIRS transmitter was designed. This device is suitable for mice and human measurements and has the purpose of designing a device used in the whole medical researching process.

3.1. LED switching system

The first step of the creating process of this new NIRS device was the design of the switching system of the light emitters. This system emits 4 different wavelengths and recovers them accurately.

As shown in Figure 8, MEMS are the most commonly used devices to switch the different sources in NIRS prototypes and commercial NIRS. Microelectronic and microelectromechanical systems are employed to switch different light sources by using micro-mirrors that reflect light beams. The direction in which the light beam is reflected changes when the mirror rotates to different angles, allowing the input light to be connected to any output port [17].

This kind of devices have certain strengths such as the 10-30 msec switching time, the compact low-loss switches on any scale and the possibility of switching optical signals without converting them into electrical signals. MEMS switches are worthwhile components unlike other optical switches (Liquid crystal, thermo-optic, semiconductor optical switches…), but they are still expensive devices (~1000€ Opneti.Co). Because of that, it would be convenient to find a more economical solution for the NIRS device with the purpose of designing a cheap and efficient near-infrared spectroscopy.

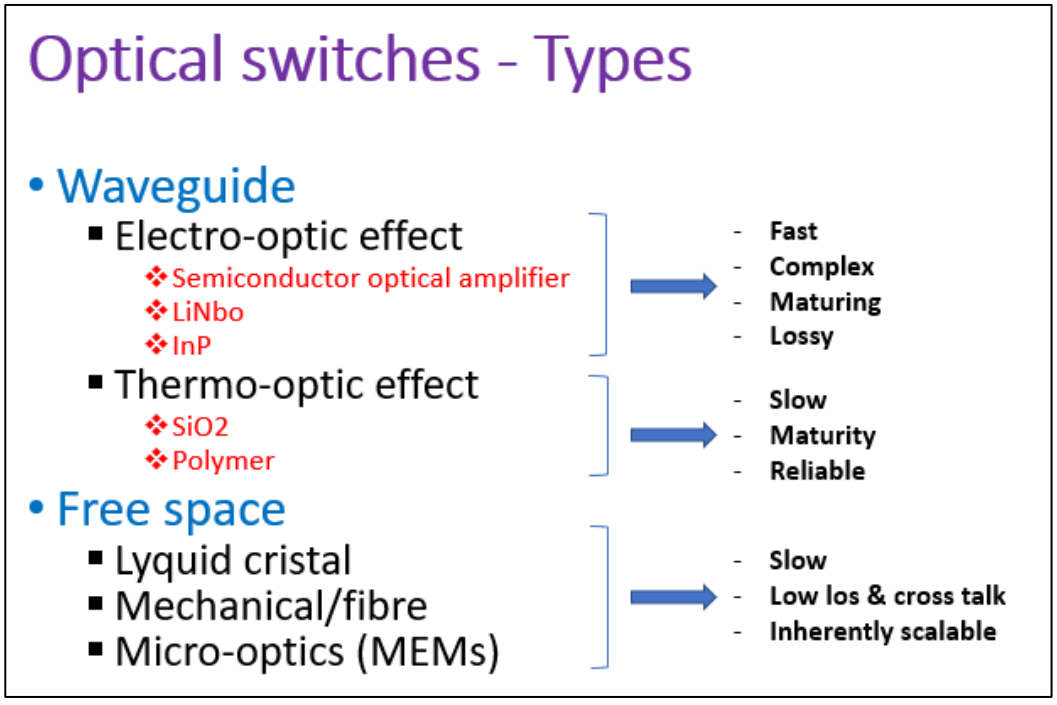

Figure 8: Types of optical switching [18]

3.1.1. Led switching system design

As already mentioned, a switching system that allows changing different light sources in NIRS device was designed. This system had to be economical, efficient and small. The proposal is shown in Appendix 1.

The components of the system are described below providing full information of how they work and their functionalities.

3.1.1.1. NE555

NE555 is a precision timing circuit that produces accurate time delays. This timer is used to generate an accurate clock signal of at least 4 kHz through a A-stable Operation that worked as the switching frequency of the system.

As can be seen in Figure 9, the circuit consists mainly of 2 resistors and 1 capacitor. Capacitor C charges through Ra and Rb and discharges exclusively through Rb - a potentiometer to adjust frequency. Subsequently, the duty cycle is controlled by the values of Ra and Rb. This A-Stable connection leads to the charge and discharge of capacitor C between the threshold-voltage level and the trigger-voltage level.

To adjust the clock signal frequency, the pertinent resistors and capacitor were selected following this formula:

$$Frequency = \frac{1.44}{(Ra + 2Rb)C} \tag{3}$$

$$Ra = 39kOhm$$
$$Rb = 30kOhm$$
$$C = 0.01uF$$

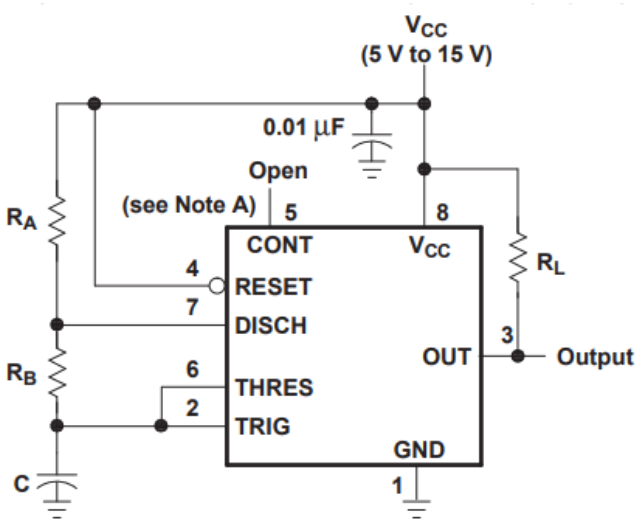

Figure 9: NE555 A-Stable configuration

The modification of the clock signal of the system and, consequently, the work frequency of NIRS, depends on the value of the resistors and the capacitor. Just by

adding a potentiometer on this schematic, it could reach a scalable frequency system. This piece of information is essential since different frequencies are applied with different purposes and in cases such as mice measurements, human patients, etc.

3.1.1.2. IC 4017

This integrated circuit is a CMOS decade counter that counts from zero to ten and whose outputs are decoded.

The pulses generated as an output of the NE555 are generated as an input to the 4017 through PIN14. When a clock pulse is received by the clock input, the counter increases the count and activates the corresponding output PIN. This ON-OFF switching of the outputs repeats on every clock pulse producing a circling effect. In this case, outputs 2, 4, 10, 5 (every second output of 4017) were selected to achieve delays among LEDs turning on and off. Thereby, the channels can be divided in the receiver and LEDs overlapping eliminated.

As shown in Figure 10, some additional pads are needed in the 4017 outputs to get synchronous signals from the circuit.

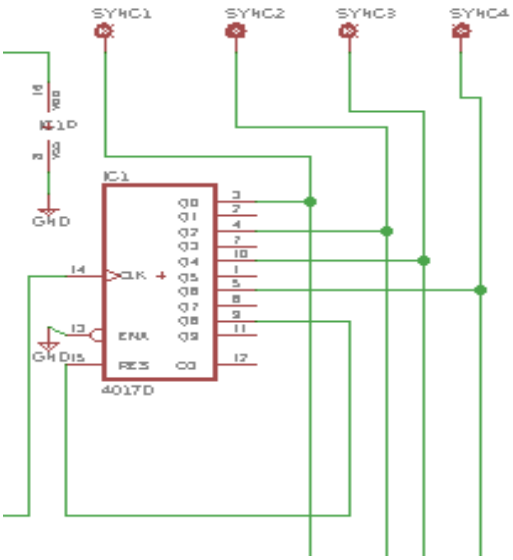

Figure 10: PIN connections of 4017 from Eagle schematic

3.1.1.3. ADG841

Another main component of the switching circuit is ADG841 single SPST switch. These high current capability switches are indispensable due to the low output current of the IC4017. For this reason, this output signal of IC4017 was used as a logic control input of ADG84. Therefore, a 4 ADG841 (1 for each output of IC4017) was needed.

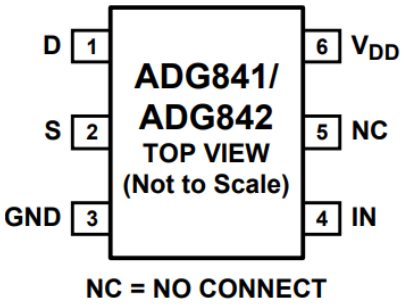

Figure 11: ADG841 PIN distribution

As it shall be explained later, the Vdd supply voltage was extracted from the 12V general supply voltage making use of a voltage regulator to get 3.3 V for the Vdd.

ADG841 drain gate was added to supply current for switching LEDs, as needed. For this purpose, a voltage regulator and potentiometers were attached. Once the potentiometer was connected to the drain, the regulation of the current that supplies LEDs was doable. This regulation avoids overpowering and regulates the diverse electrical and optical characteristics.

Lastly, the source gate was connected directly to the LEDs sources.

3.1.1.3. LM1117

This device is a low dropout voltage regulator with a 1.2V dropout at a load current of 800mA. The regulator output voltage can be adjusted between 1.25 and 13.8V.

The main purpose was to create a more stable voltage supply signal in order to feed the board integrated circuits.

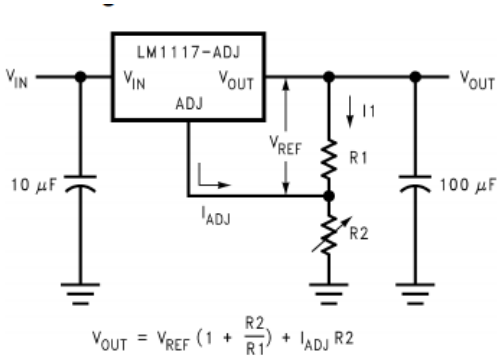

Figure 12: Adjustable output voltage set-up

3.1.2. Realization of the PCB

The next stage was the design of the pcb through Eagle software.

The board with the correspondent components footprints is shown in Figure 13.

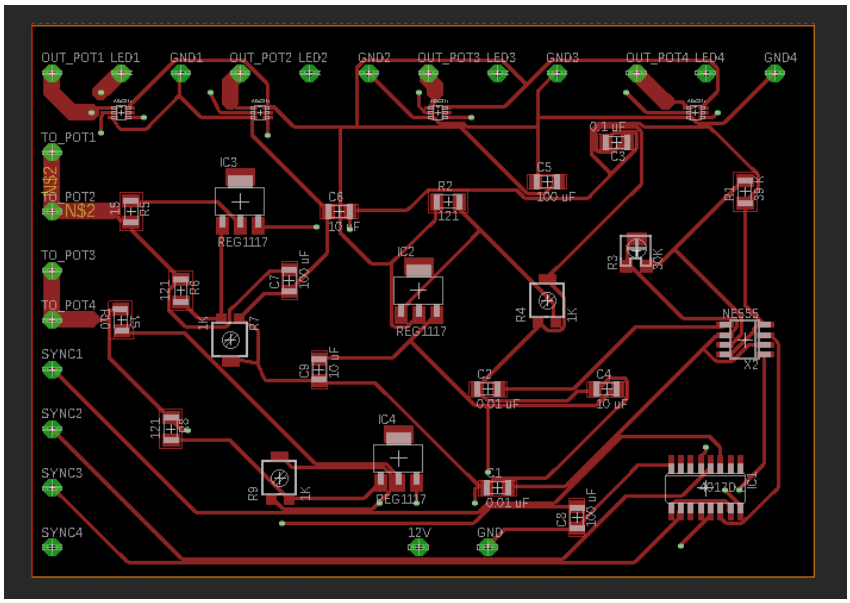

Figure 13: Eagle board of switching system

The pcb board is approximately 10.8 x 7 cm. The output pins, potentiometers pins and synchronous signal pins that cover half of the board sides are the cause of its size. An Eagle auto-routing tool was employed for routing. Moreover, modifications were amended on line paths and on other parameters such as line width, lines separation or isolation, along with a layer on both sides to create a ground layer that covers the board.

Respecting the realization of the board and the soldering process, it is important to mention that Fablab Oulu laboratory and instrumentation were used.

The board is made of a FR4 of 1.66 mm boar thickness and 35um thick copper traces. A pick-and-place machine and a reflow oven are responsible for the soldering process. Figure 14 shows the results.

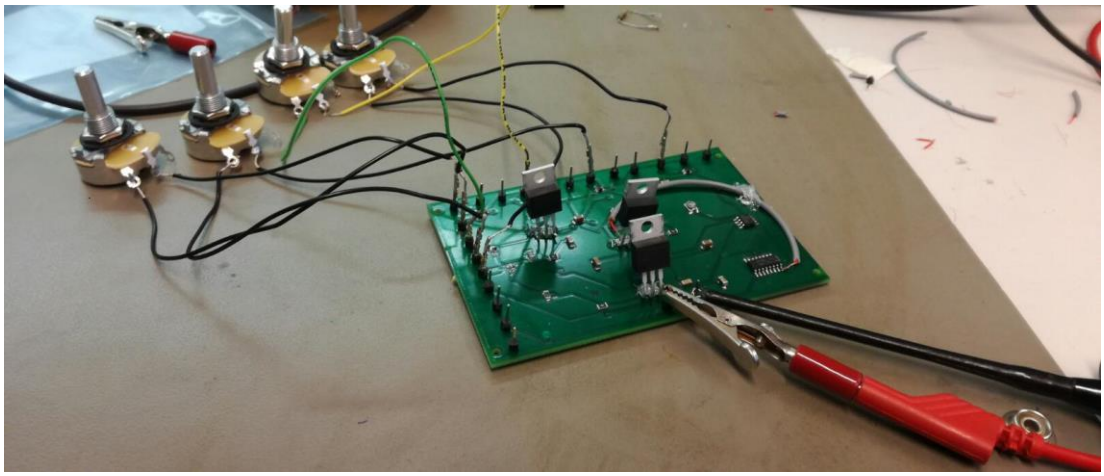

Figure 14: Final switching system board

Some modifications were amended during the soldering process. The aim was to improve some characteristics and make use of the materials and components in the laboratory. As seen in Figure 14, modified through-hole voltage regulators were used instead of SMD. Path corrections were made on the pcb board and, as a result, a

LM4017 Vdd voltage provided the voltage regulator through a physical cable and not through the PCB path developed specifically for that purpose.

3.1.3. Testing of switching system board

For the initial tests, additional synchronous pins were tested. Thus, wrong clock generator operations or a faulty decade counter could be detected without suplementary LEDs. These tests determined the proper functioning of the system.

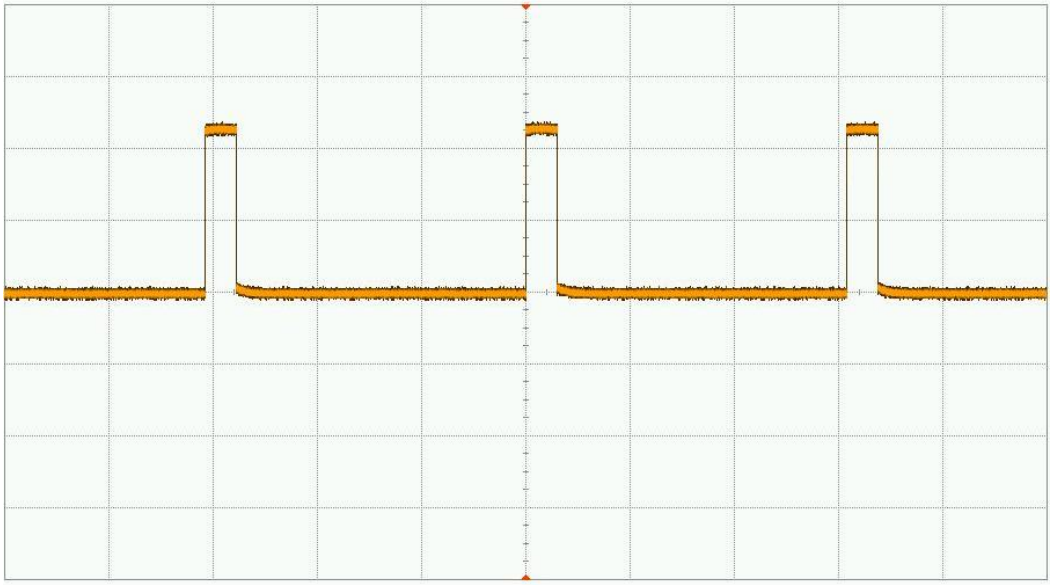

Figure 15: Tested clock signal

The clock signal plot showed a positive timer running. Its frequency reached approximately 4 kHz, which were distributed among the 10 outputs of the decade counter. The switching system operated similarly, as shown in Figures 16 and 17.

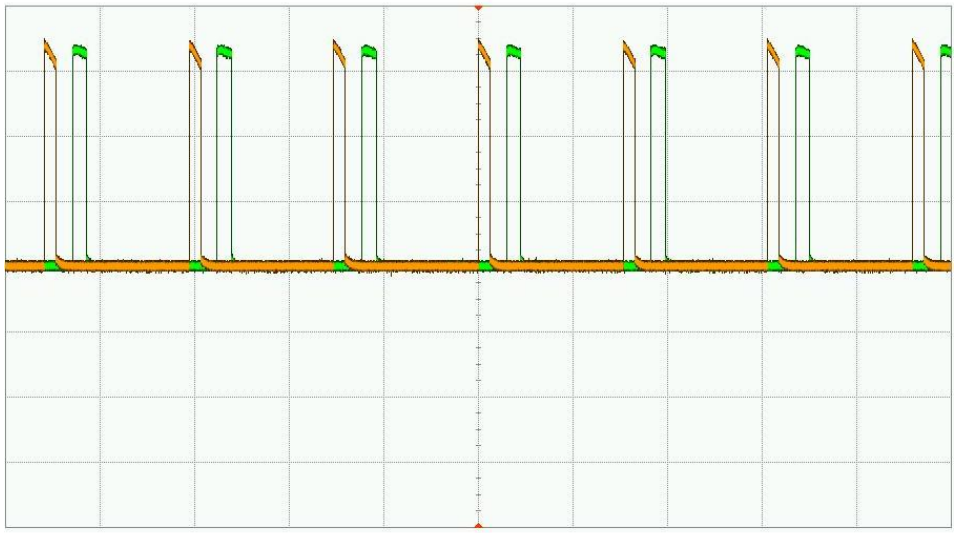

Acquisition	Sampling mode real time Normal Memory depth automatic 2000003 pts Sampling rate automatic Sampling rate 100 MSa/s Averaging off Interpolation on
Channel 1	Scale 100 mV/ Offset 1 mV Coupling DC Impedance 1M Ohm
Channel 2	Scale 100 mV/ Offset 0.0 V Coupling DC Impedance 1M Ohm
Time base	Scale 2.00 ms/ Position 0.0 s Reference center
Trigger	Mode edge Sweep auto Sensitivity normal Holdoff time 50 ns Coupling DC Source channel 1 Trigger level 171.2 mV Slope rising

Figure 16: Output of synchronous pins 1 and 2

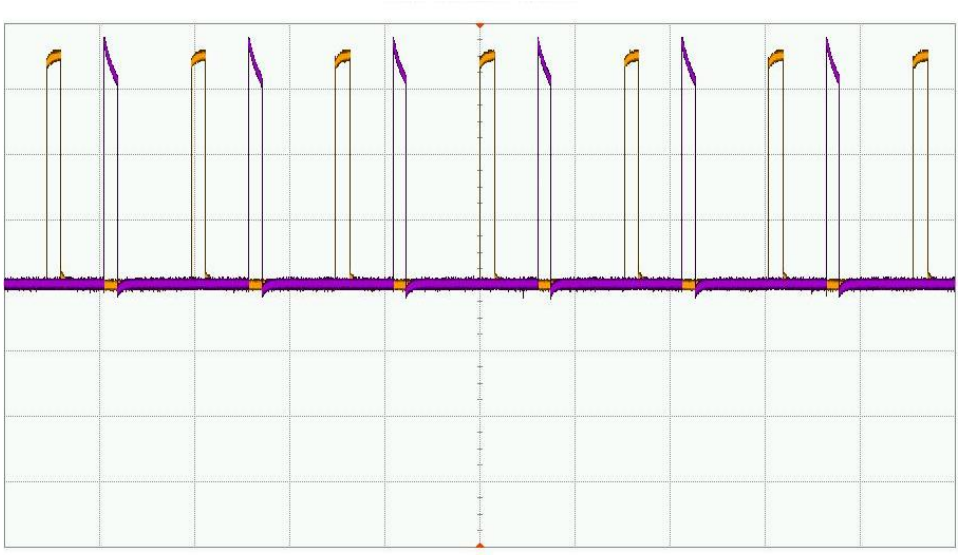

Acquisition	Sampling mode real time Normal Memory depth automatic 4000003 pts Sampling rate automatic Sampling rate 200 MSa/s Averaging off Interpolation on
Channel 1	Scale 100 mV/ Offset 1 mV Coupling DC Impedance 1M Ohm
Channel 3	Scale 100 mV/ Offset 0.0 V Coupling DC Impedance 1M Ohm
Time base	Scale 2.00 ms/ Position 0.0 s Reference center
Trigger	Mode edge Sweep auto Sensitivity normal Holdoff time 50 ns Coupling DC Source channel 1 Trigger level 171.2 mV Slope rising

Figure 17: Output of synchronous pins 1 and 3

Regarding the second test, 3 LEDs were added and light and output signals were checked by means of an oscilloscope were checked. The results are shown in Figures 18 and 19.

As can be seen in the pictures, the output pulses shape was satisfactory and the frequency of the emitters matched the planned specifications of the switching system. The peaks on the plot due to oscilloscope capture time are not relevant.

The results are visible by checking the visible-light LEDs light, or the infrared LEDs light with a phone camera.

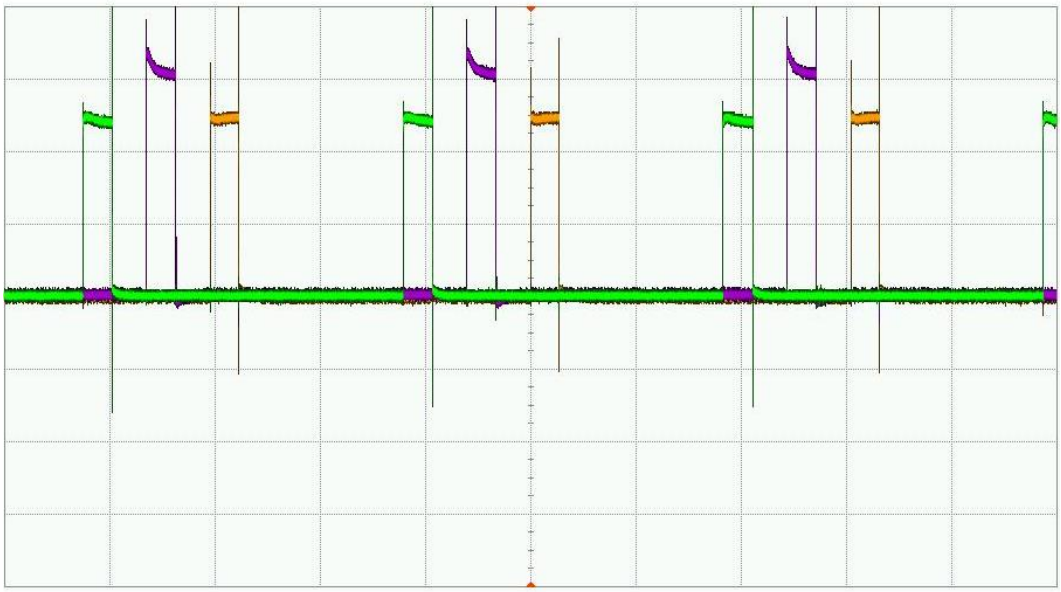

Acquisition	Sampling mode real time Normal Memory depth automatic 2000003 pts Sampling rate automatic Sampling rate 200 MSa/s Averaging off Interpolation on
Channel 1	Scale 100 mV/ Offset 2 mV Coupling DC Impedance 1M Ohm
Channel 2	Scale 100 mV/ Offset 0.0 V Coupling DC Impedance 1M Ohm
Channel 3	Scale 100 mV/ Offset 0.0 V Coupling DC Impedance 1M Ohm
Time base	Scale 1.00 ms/ Position 0.0 s Reference center
Trigger	Mode edge Sweep auto Sensitivity normal Holdoff time 50 ns Coupling DC Source channel 1 Trigger level 197.0 mV Slope rising

Figure 18: Pulses of 3 outputs of the switching system

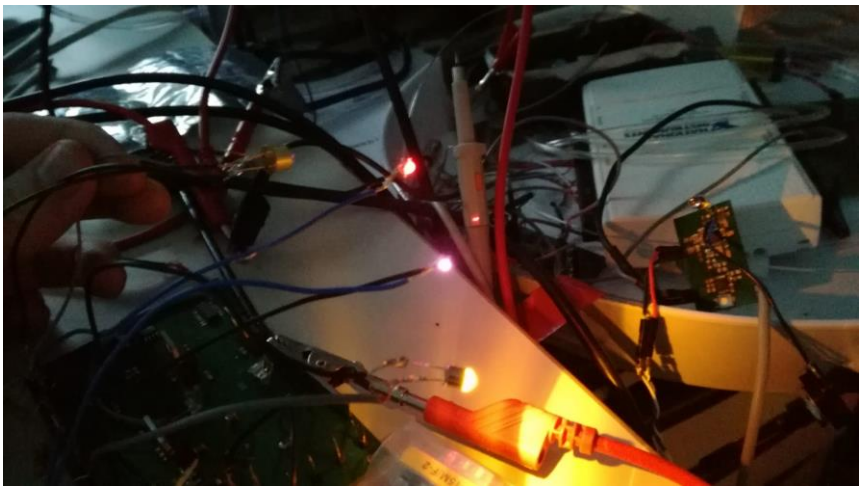

Figure 19: Lighting of LED switching system

3.2. Receiver

A receiver able to receive LEDs signals that go through the head synchronously to analyse the data was designed with a view to ensuring the proper operation of the new NIRS transmitter. The following circuit was designed by MSc. Erkki Vihriälä.

3.2.1. Receiver system

Respecting its operation, a transimpedance amplifier converts the current generated by the photodiode into voltage. Immediately after, synchronous signals from the decade counter and switches separate the different wavelengths into the different channels. After this, the voltage signal is band pass filtered by 2 Sallen Key filters and amplified by a non-inverting amplifier. The diagram of the system is shown in Figure 21.

The aim of this receiver was to filter 4 kHz frequency signals - frequency operation of the switching system. Should the operation frequency of the system change, this receiver would be modified in order to get a very accurate signal. Furthermore, if the frequency of the switching system is not as accurate as expected, the received signals could be incorrectly shaped due to a bad filtering process through the Sallen Key filters. If this were to happen, the system should be likewise modified.

The same laboratory, procedures and instrumentation provided by Fablab Oulu were utilised during the building and soldering processes.

The board was made of FR4 material of 1.66 mm boar thick and 35um thick copper traces. A pick-and-place machine and reflow oven were used during the soldering process. Schematic and final PCB boards are shown in Figures 20 and 21.

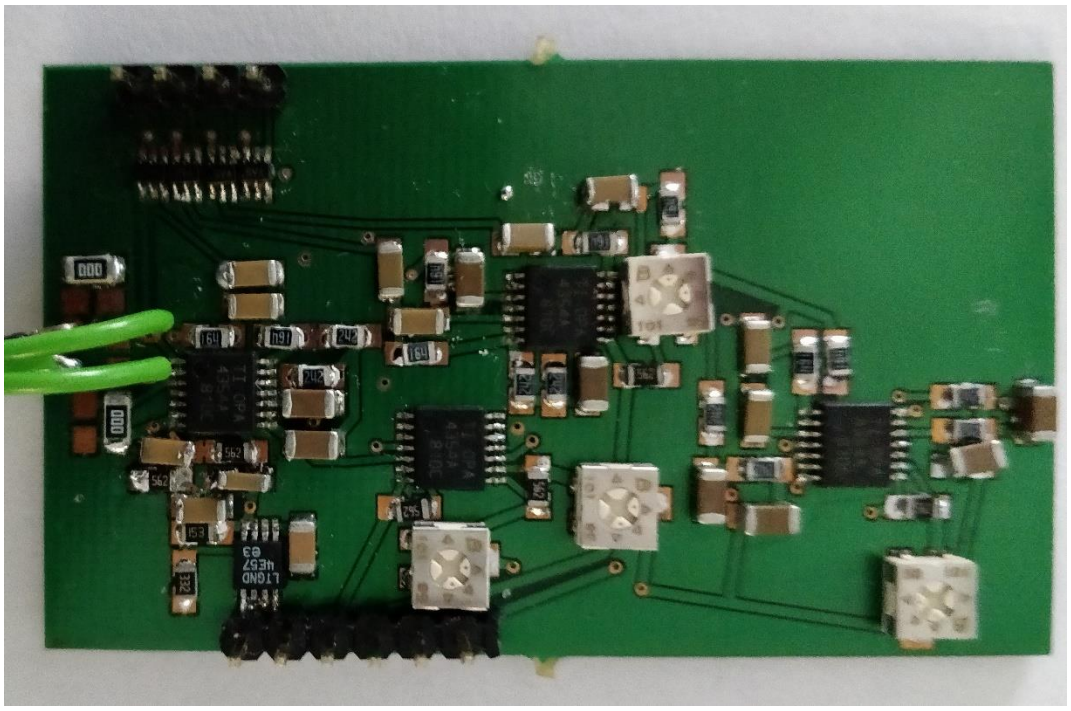

Figure 20: PCB receiver

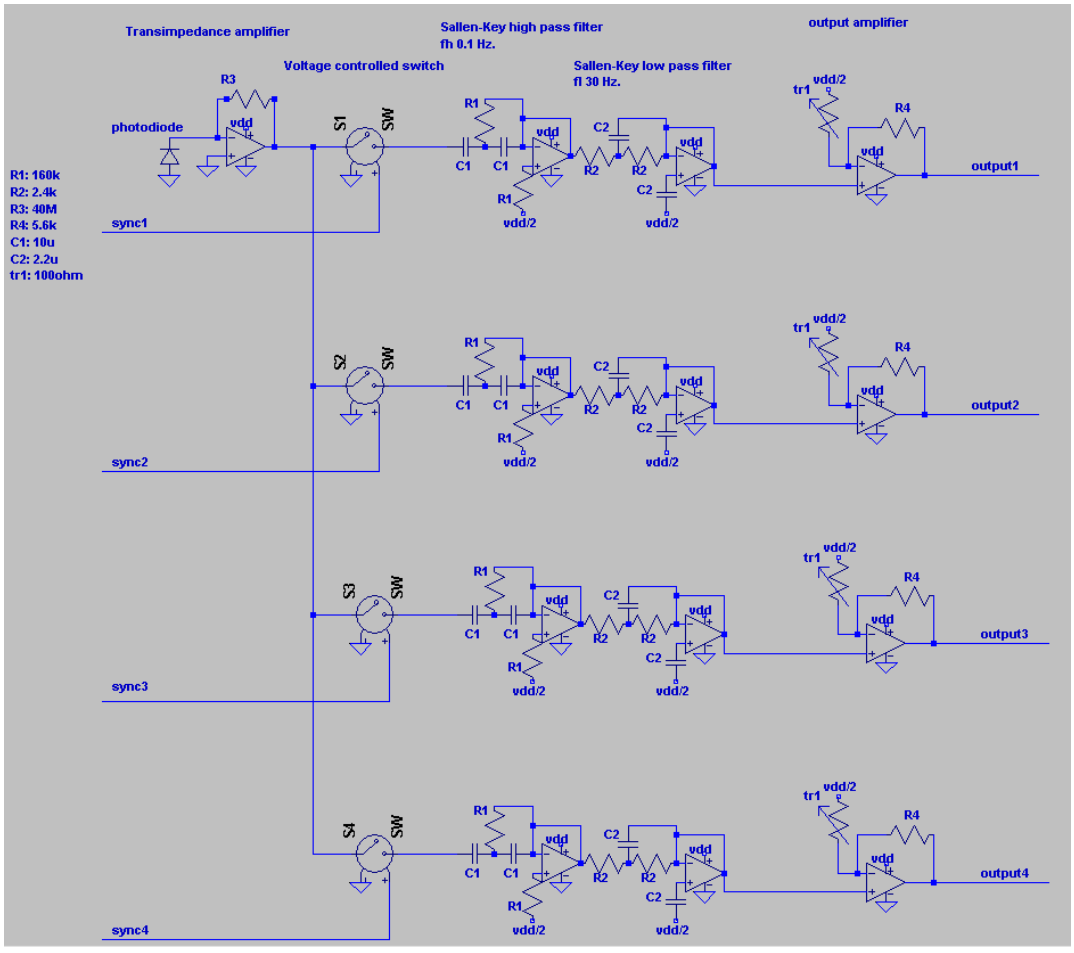

Figure 21: Diagram of receiver operation

3.2.2. Receiver system testing

Once the emitter switching system and the receiver were built, the whole system was tested. The emitters had to function properly, the photodiode had to be on and the receiver had to be connected to the data acquirement system. In order to receive the data from the system and show it in PC by some graphics, a Labview system was designed.

By running every system and focusing LEDs light on the photodiode of the receiver, the correct operation of the system was checked. The result is shown in Figure 22.

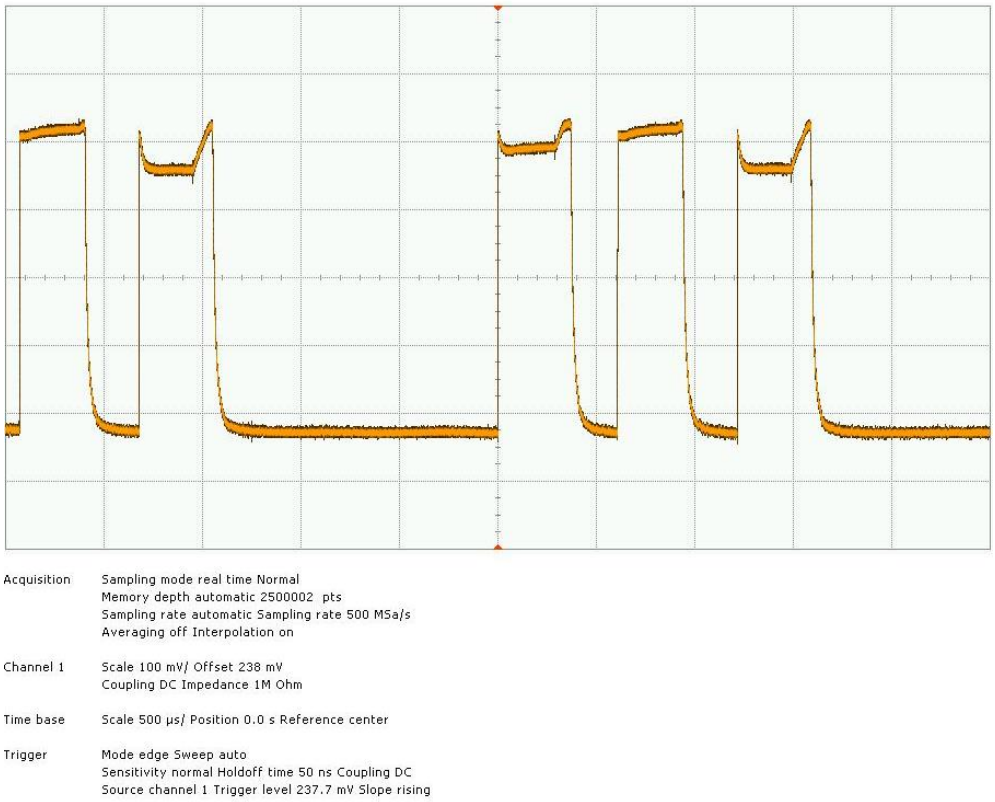

Figure 22: Received signal from NIRS system

With the purpose of knowing the results and easing the testing process, only 3 of the LEDs were used due to operational details.

Since the LEDs have different electrical and optical properties, there is a disparity of the amplitude of the peaks of the system caused by the difference among the switching system voltage pulses. Considering the voltage differences and knowing exactly how they affect the results, this would not constitute an issue for data processing.

By focusing on the shape of the signal, it may be observed that it is not ideal. This irregularity was caused by the light on the laboratory during the testing, even though the lamps were turned off, and by the fact that the receiver and the emitter are not perfectly synchronised, along with the imperfect filtering system.

3.3. Final NIRS switching system set-up

3.3.1. Set-up box building

At this stage, it was necessary to consider how to engage all the systems and boards needed for NIRS operation in just one device. Therefore, a black aluminium box of 4x10x10 inches was attached to the NIRS LED switching system, the receiver board, the data acquirement device and the PPG signal systems included in the future.

The box underwent changes in order to have a functional box and introduce the NIRS device. 5 optical fibre holes (four for LEDs emitters and one for photodiode signal of the receiver) were needed, in addition to a USB connector, a power supplying connector pass and an operational light signal space for data acquisition system. This box was built on the Workshop of Oulu University facilities.

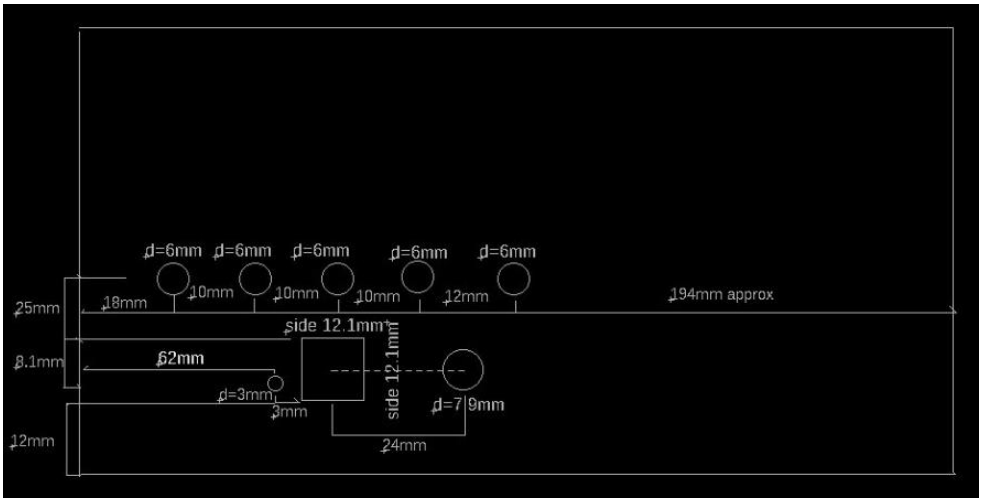

Figure 23: Non-scaled quick first sketch of box side

Figure 24: Final box side with connectors attached

Figures 23 and 24 show the initial design of a NIRS device box side and a box side with optical fibre connectors and a power supply connector.

Once the set-up box was produced, the NIRS system was attached to the board and the NIRS operation was tested.

3.3.2. NIRS switching system finger sensing

As a first step to test the definitive version of the new NIRS switching system device, finger pulse sensing needs to be performed.

The test was performed in the Optoelectronics laboratory from OPEM research group in Oulu University with a total duration of approximately 90 seconds. During the test only 2 LEDs (850nm and 600nm) were operative to ease the data acquisition and processing analysing.

In figures 25 and 26 are shown the results for samples recorded during the first 29 seconds period of the experiment:

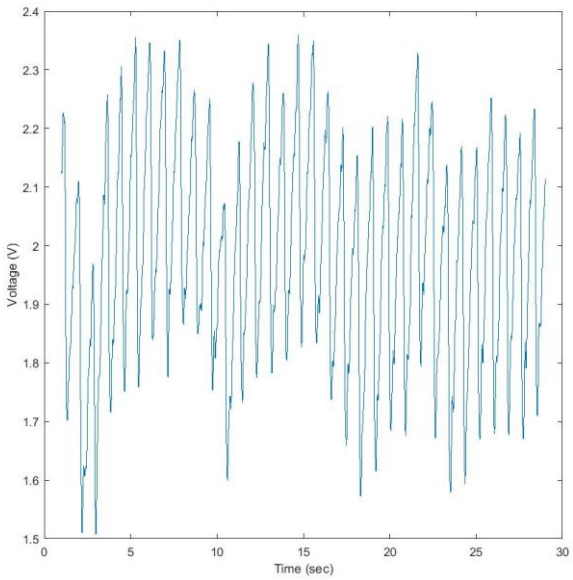

Figure 25: Voltage-time graphic for finger test using 850nm LED source

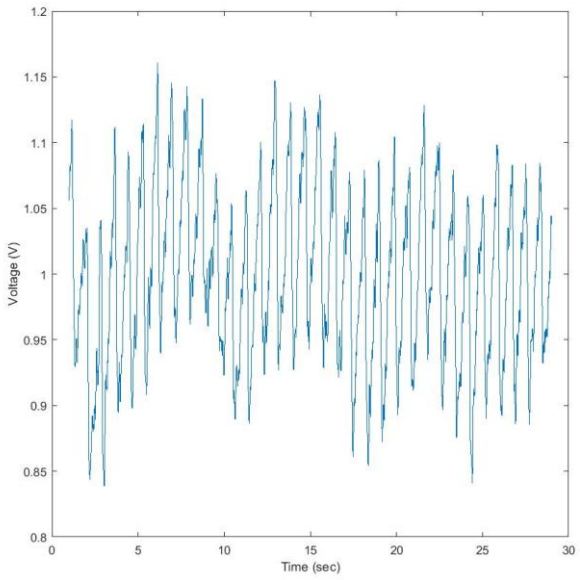

Figure 26: Voltage-time graphic for finger test using 600nm LED source

From the results it could be concluded that the switching system of the NIRS device is working properly, showing clear pulse signal for both wavelengths.

It is also shown that the voltage values recorded for 800nm LED are bigger than those recorded for 600nm. This could be due to the differences in the optical properties of the used LEDs and power variations that were commented in point 3.1.3.

3.3.3. Future testing – Mice measurements

Finally, the complete system should be future tested with mice before the application of this technique to humans.

There are some important achievements related with mice experiments and NIRS devices. One interesting article is the research work done by Seungduk Lee and her team about the cerebral hemodynamic responses to seizure in mouse brain, using simultaneous near-infrared spectroscopy and electroencephalography.

In this work, it was applied NIRS and EEG simultaneously on mice to investigate epileptic cases under pharmacologically driven seizure, gamma-butyrolactone and another substances. The research showed the following results [20]:

- Oxyhemoglobin level rises in case of GBL treated mice but not with 4-AP treated mice.
- The response to absence seizure decreases in deoxyhemoglobin.
- The phase changes between oxy and deoxyhemoglobin were reduced in GBL treated mice but not in 4-AP treated mice.
- The spatial correlation of hemodynamics increased in 4-AP treated mice but not in GBL treated mice.

Following the steps previously achieved by some research groups as the previously cited, the future lines of the new NIRS device system should be focus in testing in mice experiments before proceeding with the human testing to continue with application of new modulation techniques previously explained.

4. 3D DESIGNS FOR NIRS MEASUREMENTS

Testing the devices and taking measurements that provide realistic results are essential stages when it comes to designing imaging diagnostic systems. This project belongs to the sensitive field of the human health field and, for this reason, previous experiments had to be conducted before human testing.

In this case, a human head had to be measured with NIRS techniques, hence the creation of a phantom head prototype. Later on, a realistic phantom prototype with human electrical and optical properties was created with the purpose of taking previous measurements with the already built NIRS device. Researchers in recent years have focused on the optical field regarding NIRS devices and optical properties but, nowadays, microwave imaging systems are also being studied because of their potential. For these reasons, this thesis addresses both systems.

Additionally, new 3D printed pieces were designed and applied in biomedical studies to measure ppg signal through a NIRS device and other different body properties.

4.1. 3D printed pieces for measuring NIRS signal

Pulse Oximetry and Near Infrared Spectroscopy are the most widely applied optical techniques for tissue perfusion analysis. Pulse oximetry estimates arterial oxygen saturation (SpO2) by passing two wavelenghts of light, allowing it to determine the constant absorbers (DC) due to the pulsing arterial blood (AC). NIRS processes the attenuations of at least two wavelengths and calculates concentrations of Deoxygenated ([HHb]), Oxygenated ([HbO2]), Total Haemoglobin ([tHb]) and Tissue Oxygenation Index (TOI) [19]. The pieces facilitate the system measurements by adopting both Pulse Oximetry and NIRS principles to calculate SpO2, [HHb], [HbO2] and [tHb].

A photoplethysmograph (PPG) is a type of graph obtained through optical techniques that allow the volumetric measurement of an organ. The most commonly used technique to obtain PPG is the use of a pulse oximeter that illuminates the skin and measures changes in light absorption [21]. The heart pumps blood to the peripher with every cardiac cycle and the change in volume caused by the pressure pulse is detected by illuminating the skin with a LED light. After the measurement, the amount of light is transmitted/reflected to a photodiode. Skin blood flow can be modulated by multiple physiological systems and PPG can be used similaryly to monitor breathing and hypovolemia among other circulatory conditions [21]. PPG can be obtained from different parts of the body depending on the parameter, but the device is commonly placed on a finger tip due to its transmissive absorption.

To this aim, a 3D piece was designed. This piece could have attached up to 2 optical fibers (transmitter and receiver), makes finger measurents comfortable and is lightweight and affordable.

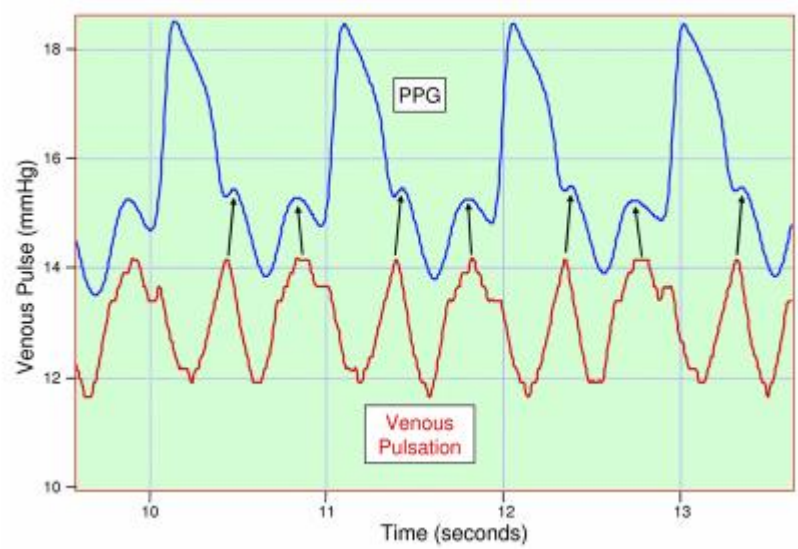

Figure 27: Example of PPG signal. Venous pulse measurement [21]

The software used for designing the 3D model was Solidworks. The results can be seen in Figure 28.

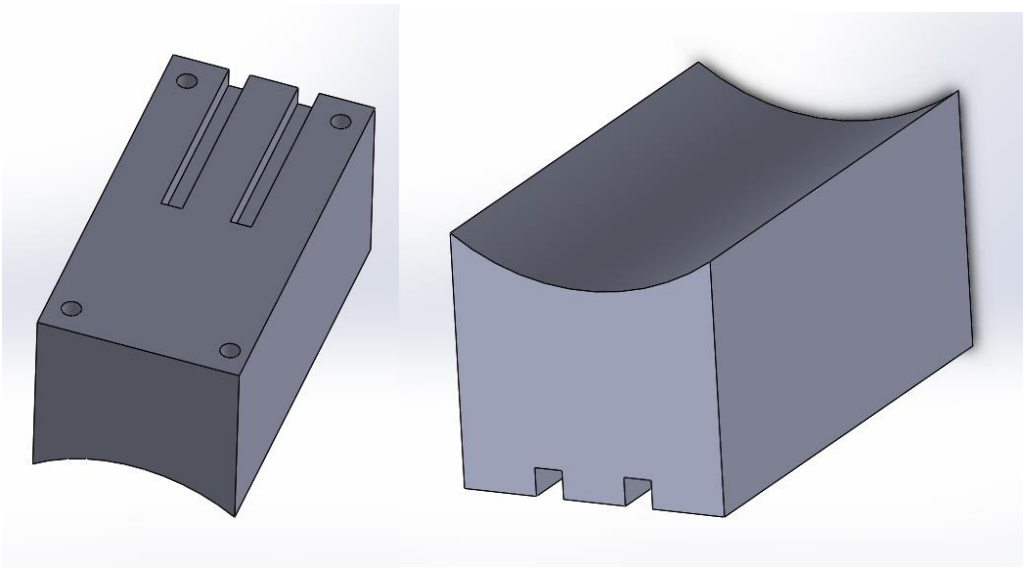

Figure 28: Front and top view of the 3D design

The piece is approximately 26x40x20 mm. Owing to the size and its properties, a Stratasys 380mc 3D printer provided by the Fablab Oulu University printed a provisional white piece. The result is shown in the following pictures.

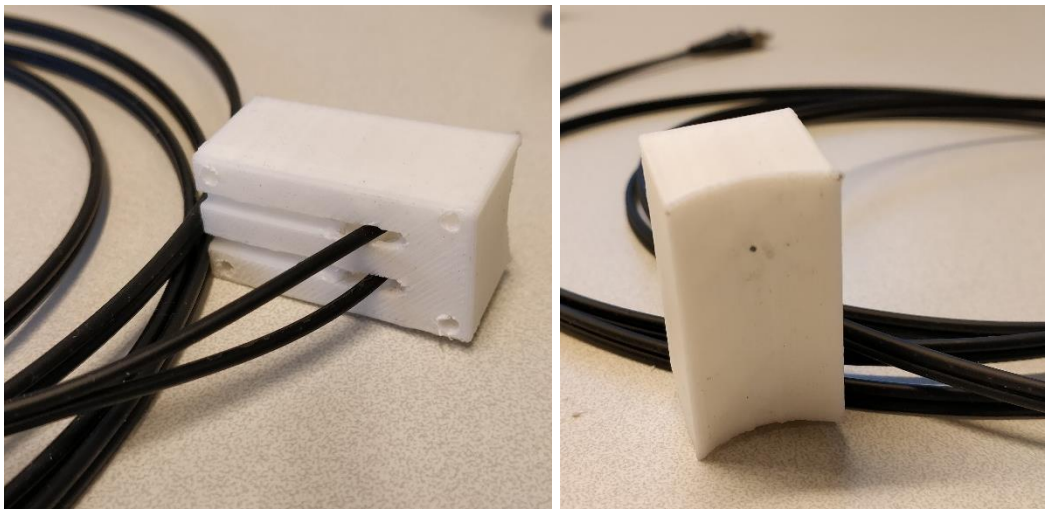

Figure 29: 3D printed design in white

After studying the operation of the system, it was clear that the material and colour used for the first prototype could become a disruption for the receiver due to the optical properties of the piece. Therefore, a second and a more comfortable to hold prototype was printed in black using ABS material. Figure 30 shows the result.

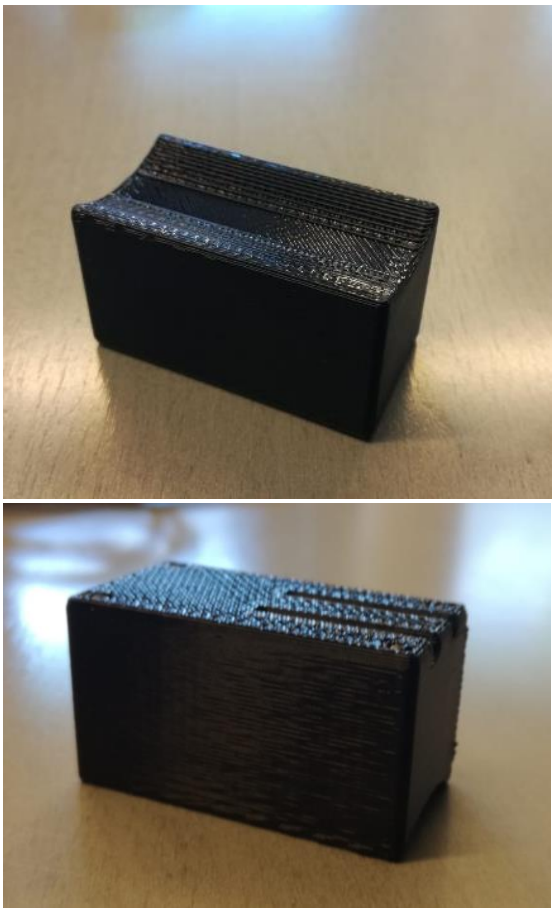

Figure 30: 3D printed design in black ABS

4.2. Phantom head

Nowadays, the state-of-the-art of phantom heads experiments focuses on optical and microwave phantoms. This field of research is not highly developed, therefore, it is essential to know the history of this field in order to approach the work correctly.

4.2.1. Microwaves phantom head review

The high contrast of the electrical properties among healthy and stroke-affected brain tissues makes clear the potential of using microwave imaging systems for brain imaging. Furthermore, low-priced and portable microwave systems could be designed for brain imaging, making it an unexploited field of research [22].

Nowadays, microwaves imaging techniques offer an alternative to the commonly and widely used techniques (X-Rays, MRI, ultrasound…). This innovative and non-invasive technique utilises nonionizing electromagnetic signals with low power on the microwave range.

Generally, microwaves imaging equipment for medical purposes includes a microwave source, a receiver, an antenna array and a switching system microwave to change elements on the array. This equipment is clearly more affordable than others and makes microwave imaging a cost-effective system. Considering that it is a portable system, it could be installed in ambulances for fast diagnosis of life-threatening conditions, among other locations. As stated above, this technique entails advantages as long as disadvantages such as the bad spatial resolution of the images obtained from these techniques [23].

Before conducting animal and human clinical trials, it was necessary to create an artificial head phantom that had the same electrical properties a human tissues across the frequency band of interest (1-4 Ghz) to test the microwave techniques.

A relevant research study of 2013 by the University of Queens reveals an economical and simple mixture to form CSF, blood, grey and white matters, as can be seen in.

	CSF	Grey Dead/Alive	White Dead/Alive	Blood
Water (mL)	150	560/570	350/364	100
Corn Flour (g)	5.45	350/286	200/185	12.8
Gelatin (g)	0	0/0	10.5/9.8	24
Agar (g)	20.2	18.5/17.7	0/0	0
Sodium azide (g)	0.15	0.56/0.57	0.35/0.36	0.1
Propylene Glycol (g)	4	0/0	0/0	0

Figure 31: Mixtures [22]

The research shows a simple, fast procedure that includes polyvinyl chloride, water, corn flour, gelatine or agar and sodium azide. It has to be mentioned that sodium azide is a sever poison that it is not allowed to be used in many Universities and laboratories as it may be fatal in contact with skin or if it is swallowed, been able to show symptoms even in minutes. So the use of this kind of azide should be approved by authorized staff under several security conditions.

Firstly, the polyvinyl chloride is shaped as a human skull and used as a phantom shell. Diverse materials representing CSF, grey matter, and white matter were introduced into the skull and a thin layer representing the scalp covered the outer part of the skull. Lastly, the phantom head is covered with a wig mimicking hair [22].

On the one hand, Grey and White matters were a mixture of corn flour and ¾ of the volume quantity of water in a 2-L beaker at ambient temperature. On the other hand, gelatine was poured slowly while stirring ¼ volume quantity of water and the mixture was heated gradually from 90 to 95 ºC. When the mixture was cold, sodium azide that serves as an antibacterial was added with the aim of extending the life of the phantom. Lastly, the corn flour syrup was heated gradually and stirred the gelatine solution at a very low heat obtaining a gelatinous mixture [22].

The next step was to create CSF and blood. Firstly, the propylene glycol was mixed with water at ambient temperature and heated gradually. Next, the gelatine was gradually added and stirred from 90 to 95ºC. When the mixture cooled down, it was mixed with the sodium azide mixture and small pieces of corn flour stirred on a low heat [22].

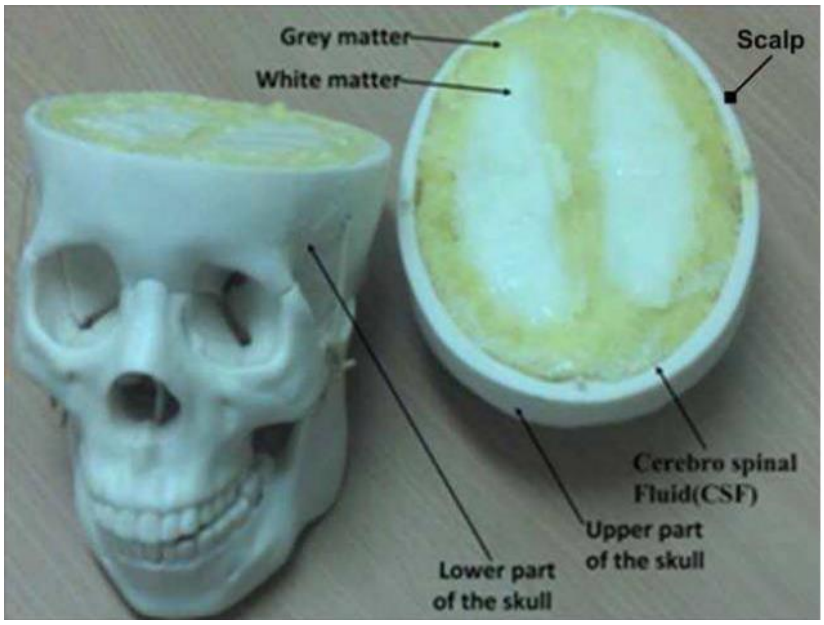

Figure 32: Final phantom head [22]

4.2.2. Optical phantom head review

Regarding optical phantom heads for medical purposes, the prototypes are not as developed as microwave dummies. The optical properties of the human head are not easily copied and, therefore, this stage of the research was not as rapid as desired.

One of the most important projects on this field was implemented by researches of the Oulu University, headed by Vesa Korhonen and Teemu Myllylä. In this project regarding light propagation in NIR Spectroscopy of the human brain, a prototype of optical human-head-layers phantom was built and tested.

In this study, a T1-weighted MPRAGE 0.9mm voxel size anatomical magnetic resonance image from a real subject was used to obtain a head structure for the

fabrication of the phantom, identifying subcutaneous tissue, bone with marrow, cerebrospinal fluid, grey matter and white matter. The first step was to construct a transparent medium host of polyvinyl chloride plastisol (PVCP) adding zinc oxide (ZnO) that simulates scattering effect [24]. The calculated properties for each layer are shown in Figure 33.

Layer	L, mm	μ_s', 1/mm	μ_a, 1/mm	μ_s, 1/mm	g	n
skin	3	1.44	0.002	7.2	0.8	1.44
skull	10	1.5	0.002	7.5	0.8	1.44
CSF	2	0.00001	0.0001	0.001	0.99	1.41
grey matter	4	2.4	0.002	12	0.8	1.44
white matter	20	7.8	0.002	39	0.8	1.44

Figure 33: Thickness of the tissue layers and optical properties at 900nm [24]

After a 15-minute sonication, the host medium with ZnO particles was poured into the metal cuvettes and baked for 70 min in a preheated oven (180 º C). This procedure enables the creation of layers of different thicknesses and shapes. The phantom created by this research group was made up of 5 layers that mimic a human skin, skull, cerebral fluid, grey matter and white matter [24]. The surface morphologies of the phantom head were shaped similarly to the human brain layers the magnetic resonance image showed. Figure 34 shows a realistic human head mould of metal.

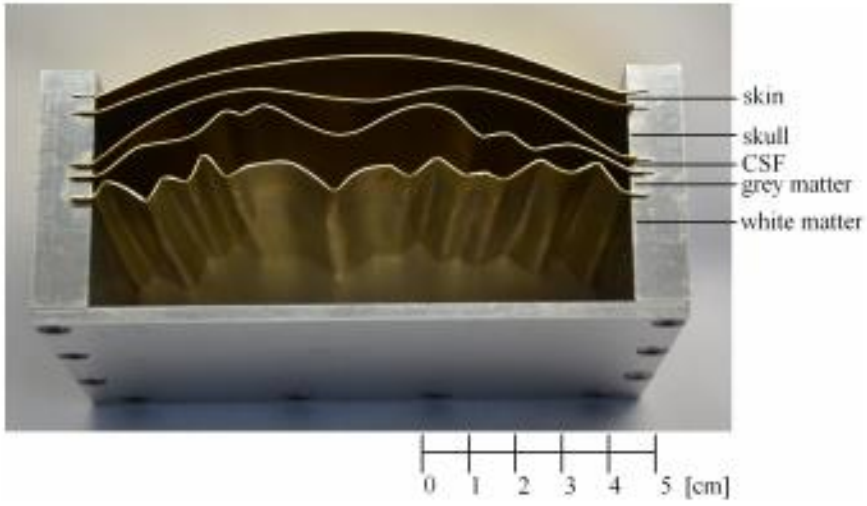

Figure 34: Multilayer mould for head-mimicking phantom [24]

4.2.3. Phantom head prototype

Phantom heads were built to mimic a human head structure and to test previously tested techniques before performing human clinical trials. Therefore, scaled realistic human head using 3D printing techniques were developed and imaging techniques were scanned.

For printing a 3D piece, a 3D editable model was essential to start the fabrication process. In order to achieve it, Creaform GoScan 3D laser scanner software shaped the human head [25]. After the scan, this design was converted into STL format. STL format is an assisted per computer format (CAD) that defines 3D objects including additional information - textures, colour or physics. This format requires to triangle the 3D design, technique used by 3D printers. The original scanned head was modified using Solidworks software to hollow equiespatially, to re-scale, to get the technically needed piece and to avoid wasting material and budget.

A Stratasys 380mc 3D printer provided by the Fablab Oulu University printed the 3D STL format file made of ABS material. The results are shown in following pictures.

Figure 35: Original human head 3D model [25]

Figure 36: 3D printed human head

By using this prototype as a mould, preliminary results in biomedical testing could be achieved. Nevertheless, a more accurately shaped head with more accurate microwave and optical properties could be built once some modifications are amended. Besides, the human layers should be accurately analysed in order to get results as accurate as possible.

5. DISCUSSION

In this thesis, it has been designed and built a functional, simple and affordable NIRS switching system based in commercial components as timer 555, decade counter 4017 and high power LED sources. This system has been designed in order to be able for being tested with both human and mice, so it is possible to be frequency escalated with a simple potentiometer circuit.

It was also manufactured a suitable setup box designed to include all the necessary hardware used for a complete NIRS system that will include also the designed transmitting and receiving system.

The NIRS transmitter has been finger pulse tested achieving successful results, being the implementation into mice measurements, one of the main future lines of the project.

As one of the main objective of the thesis, 3D printing techniques have been implemented in order to ease some biomedical studies. Optical finger optodes made by black ABS material were manufactured and tested in OPEM research group laboratories.

3D printed realistic scaled phantom head was designed and printed in order to able to start making NIRS measurements with plastic material, with known properties, as a previous step to test the NIRS techniques with realistic optical known properties phantom head.

6. SUMMARY

As it has been discussed, neuro-investigation has become of great interest in the medical researching community. Focusing in brain diseases and the early detection of these, NIRS techniques have been a great advance, being the perfect complement of the traditional neuroimaging techniques.

This is why creating new techniques, both manufacturing and technological, to achieve a wide implementation of NIRS devices in most of the medical centres around the world, is of great relevance.

It has been exposed the current NIRS state-of-art and NIRS-fMRI techniques to establish the basis of the hemodynamic responses studies of brain activity.

Once it is known the current NIRS state-of-art, it has been explained the different detection methods that are currently in used in NIRS systems, focusing this study in frequency domain detection using 4 possible different wavelengths.

It has been designed and built a simple and affordable transmitter mainly based in a timer NE555, commercial decade counter 4017 and 4 high power LED sources. A Sallen-key filtering based receiver has also been designed and implemented to be included in the set up box that will contain the complete NIRS device.

The whole system has been finger pulse tested achieving successful results that show a properly performance of the switching system.

As mentioned before, implementing new 3d printing techniques in medical researches is a great step in the process of easing and providing realistic results in this sensitive field. It is because of this that it has been designed and built a new 3d printed piece to be used for NIRS experiments in combination with PPG measurements that make finger sensing comfortable, lightweight and affordable.

Finally, it has been designed and 3d printed a realistic scaled phantom head that will be the first step in the process of manufacturing a testing phantom head with properly optical and microwave properties that will allow to make NIRS experiments with a high accuracy results.

7. REFERENCES

[1] Marco Ferrari, Valentina Quaresima. A brief on the history of human functional near-infrared spectroscopy (fNIRS) development and fields of applications. 2012.

[2] Marie-Jeanne Bertrand, Philippe Lavoie-L'Allier and Jean-Claude Tardif. NIRS: A novel tool for intravascular coronary imaging. 2017.

[3] Chance, Zhuang, Unah, Alter, Lipton. Cognition-activated low-frequency modulation of light absorption in human brain. 1993.

[4] H. Obrig, C. Hirth, J. Ruben, U. Dirnagl, A.Villringer, H. Wabnitz, D. Groseni ck, H.Rinneberg. Near-infrared spectroscopy in functional activation studies: new approaches. 1996.

[5] R. Cubeddu, A. Pifferi, P. Taroni, A.Torricelli, G. Valentini. A compact tissue oximeter based on dual-wavelength multichannel time-resolved reflectance. 1999.

[6] Tommi Noponen. Instrumentation and methods for frequency-domain and multimodal near-infrared spectroscopy, doctoral dissertation, Department of biomedical engineering and computational science. 2009.

[7] Davies, Zhangjie, Clancy, Lucas, Dehgani, Logan and Belli. Near-Infrared Spectroscopy in the monitoring of adult traumatic brain injury: A review. 2015.

[8] N. Nagdyman, P. Ewert, B. Peters, O. Miera, T. Fleck, and F. Berger. Comparison of different near-infrared spectroscopic cerebral oxygenation indices with central venous and jugular venous oxygenation saturation in children. Paediatr. Anaesth. 18:160-166. 2008.

[9] Hyeonmin Bae. Basic principle and practical implementation of near-infrared spectroscopy (NIRS). 2015.

[10] Siana Jones, Scott T. Chiesa, Nishi Chaturvedi, and Alun D. Hughes. Recent developments in near-infrared spectroscopy (NIRS) for the assessment of local skeletal muscle microvascular function and capacity to utilise oxygen. 2016.

[11] http://www.opennirs.org/docu/02_open_NIRS_docu_StateOfTechnology.pdf

[12] Rebecca Re, Ileana Pirovano, Davide Contini, Lorenzo Spinelli and Alessandro Torricelli. Time Domain Near Infrared Spectroscopy Device for Monitoring Muscle Oxidative Metabolism: Custom Probe and In Vivo Applications. 2017.

[13] Assländer J1, Zahneisen B, Hugger T, Reisert M, Lee HL, LeVan P, Hennig J. Single shot whole brain imaging using spherical stack of spirals trajectories. 2013.

[14] T.Myllylä, V.Toronov, J.Claassen, V. Kiviniemi, V.Tuchin. Near-Infrared Spectroscopy in Multimodal Brain Research. 2016.

[15] Vesa Korhonen, Tuija Hiltunen, Teemu Myllylä, Xindi Wang, Jussi Kantola, Juha Nikkinen, Yu-Feng Zang, Pierre LeVan, and Vesa Kiviniemi. Synchronous

Multiscale Neuroimaging Environment for Critically Sampled Physiological Analysis of Brain Function: Hepta-Scan Concept. 2014.

[16] Vesa Kiviniemi, Vesa Korhonen, Jukka Kortelainen, Seppo Rytky, Tuija Keinanen, Timo Tuovinen, Matti Isokangas, Eila Sonkajarvi, Topi Siniluoto, Juha Nikkinen, Seppo Alahuhta, Osmo Tervonen, Taina Turpeenniemi-Hujanen, Teemu Myllyla, Outi Kuittinen, Juha Voipio. Real-time monitoring of human blood-brain barrier disruption. 2017.

[17] Mohd Nazir. Optical Switches. 2013.

[18] Professor Z. Ghassemlooy. Optical switches. School of Computing engineering of University of Northumbria. 2016.

[19] T.Y. Abay, P.A. Kyriacou. Investigation of photoplethysmography and near infrared spectroscopy for the assessment of tissue blood perfusion. 2014.

[20] S.Lee, M.Lee, D. Koh. Cerebral hemodynamic responses to seizure in the mouse brain. Simultaneous near-infrared spectroscopy-electroencephalography study. 2010.

[21] A2Kafir. Photoplethysmograph. 2001.

[22] Beada'a J. Mohammed and Amin M. Abbosh. Realistic head phantom to test microwave systems for brain imaging. 2013.

[23] Rohit Chandra, Ilangko Balasingham and Ram M.Narayanan. Medical microwave imaging and analysis. 2018.

[24] Vesa O. Korhonen, Teemu S. Myllyla, Mikhail Yu. Kirillin, Alexey P. Popov, Alexander V. Bykov, Anton V. Gorshkov, Ekaterina A. Sergeeva, Matti Kinnunen, and Vesa Kiviniemi. Light Propagation in NIR Spectroscopy of the Human Brain. 2014

[25] https://www.thingiverse.com/thing:209088 , jsteuben, 2013.

8. APPENDICES

Appendix 1. Switching system schematic